SCIREA Journal of Physics
ISSN: 2706-8862
http://www.scirea.org/journal/Physics
February 12, 2022
Volume 7, Issue 1, February 2022
https://doi.org/10.54647/physics14409

Comparative study of the performances of opaque and transparent patch antennas

A. Sissoko[1,2], A. Chousseaud[2], T. Razban[2], M. Brunet[2], S. Ginestar[2], B. Diourté[1]

[1] Institut d'Électronique et des Technologies du numéRique (France).

[2] Université des Sciences des Techniques et des Technologies de Bamako (Mali).

Corresponding Autor: Abdoulaye SISSOKO, abdoulaye.sissoko@isamali.org

Abstract:

The performances of two microstrip patch antennas with low visual impact are presented in this paper and compared to an opaque solution. These consist in a copper film deposited on a Borofloat 33 glass substrate through a thin titanium gripping layer. The mesh is obtained by wet chemical etching. Antennas differ by the dimensions in the ground plane mesh pattern. The opaque antenna only consists of a full copper deposit. The transparency work was mainly carried out on the ground plane as it is the largest area available. Specific attention is paid to optical transparency in the visible light spectrum, sheet resistance and electromagnetic performances in the [2.8; 3GHz] bandwidth. They are measured in each case, compared and discussed. Both simulations and measurement results show good performance, especially the antenna with the most transparent ground plane: A high level of optical transparency of almost 73%, coupled with a sheet resistance of less than 0.028 Ohms/sq and a gain of about 3.22dBi at 2.8GHz, slightly higher than the gain of the reference opaque antenna of about 2.66dBi at 2.99GHz. The opaque reference antenna has a bandwidth of 1.30 GHz while those of the

transparent antennas are about 1.60 GHz and 2.10 GHz (S_{11}< -10dB). This solution presents a real interest for low cost integrated and discrete antenna solutions in ISM band.

Keywords: Conductor meshed, Optical transparency, radiation pattern, transparent antenna

I. Introduction

In recent decades, the development of personal, wireless, interactive communication solutions and, more recently, Internet of Things (IoT) for example have led to the proliferation of communication systems and generated new needs for compactness. However, depending on the frequency bands involved, antenna dimensions can be one of the main obstacles in transceiver designs. The search for antenna compactness very often leads to a significant decrease in the performance of the antenna whether bandwidth or gain. It is then necessary to make the antennas discrete in a different way, including making them as transparent as possible.

It is then necessary to jointly use conductors and dielectric materials whose nature or geometry will make it possible to obtain this transparency effect. With regard to conductive materials, there are two solutions to achieve optical transparency : Using a mesh conductor or using an inherently transparent conductor [1]. In this last case, conductive transparent oxides (CTO) are increasingly commonly used [2]. They are widely used for transparent Electronics due to their ability to exhibit high optical transparency (OT) and high electrical conductivity. The most widely used is Tin-doped Indium oxide (ITO): Sheet resistance is about 10Ω/square and optical transparency around 90% [3] but ITO is fragile and expensive. Multilayer CTO technology (CTO/metal/CTO) reaches lower sheet resistances : For the multilayer ITO/Ag/ITO, it's around 7Ω/square for a transparency around 95% [4]. IZTO/Ag/IZTO is even more interesting [5] due to its flexibility and low manufacturing cost. However, this technology does not allow to achieve sheet resistances lower than 1Ω/square while preserving a high optical transparency.

In this context, we propose a new low-cost technological solution to achieve a good compromise between sheet resistance and optical transparency in the visible domain. Copper/titanium films are deposited on glass substrates by radiofrequency cathode sputtering. The mesh structuring of these bilayers by photolithographic chemical etching helps to further

increase transparency. This technology remains quite inexpensive thanks to the use of easily accessible materials as well as plastic masks for the antennas' realization.

In this work, the rules of antenna sizing and the technological process are presented. Two antennas have been designed; they differ in the dimensions of the mesh pattern of the ground plane. Indeed, the transparency work was mainly carried out on the ground plane because it is the bulkiest area of the antenna and therefore the most visible. An opaque antenna has also been designed to serve as a reference, it consists only of a complete copper deposit on each side of the glass substrate. Specific attention is paid to optical transparency in the visible light spectrum, sheet resistance and electromagnetic performances in the [2.8; 3GHz] bandwidth. They are measured in each case, compared and discussed.

II. Design and simulation

Simulating an opaque antenna is straightforward while simulating a mesh antenna is a bit more complex: It requires a very powerful computer (Random Access Memory 190Go) with a very long computation time (48h to 72h depending on the structure).

The dimensioning principle is to size the mesh antenna from a full-film antenna. In a full layer antenna, sheet resistance is linked to its thickness e and conductivity σ by (1). From the grid pitch p, the grid width s and the grid thickness e, the sheet resistance of the grid antenna $R_s^{'}$ can be calculated from that of the solid layer, R_s by (2) *[6]*.

$$R_s = \frac{1}{e.\sigma} \tag{1}$$

$$R_s^{'} = \frac{p}{s} R_s = \frac{p}{s} \frac{1}{e.\sigma} \tag{2}$$

Subsequently, it remains to define the new corresponding thickness e' such as $R_s^{'} = \frac{1}{e'.\sigma}$ (3). We then obtain a mesh antenna of thickness e with the same sheet resistance as the opaque antenna of thickness e'. The two mesh antennas presented in this paper were sized in this way.

The two antennas have been designed on the same 1.1mm thick borofloat 33 glass substrate with a loss tangent of 0.007 and a dielectric permittivity of 4.5 *[7]*. The chosen resonance frequency is approximately 3 GHz and the study was performed using Ansoft's HFSS software.

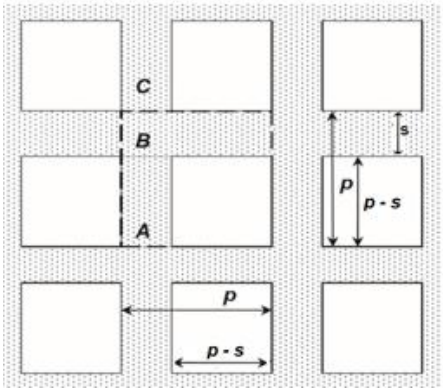

Figure 1. Mesh models

III. Antenna's fabrication Process

A) Metal Film Deposition

Thin layers of titanium (Ti) and copper (Cu) are deposited on a Borofloat33 glass substrate by radiofrequency (RF) magnetron sputtering technique at room temperature. The parameters governing the deposition of thin films by sputtering are:

- the pressure of the partial gas;
- the composition of the partial gas;
- the power applied to the target;
- the bias voltage of the substrate holder;
- the current density;
- the angle of incidence of the bombardment particles and
- the presence or absence of magnetic fields.

The work begins with pumpting at a pressure of 5.10^{-5} mBar. Then comes stripping for 3 minutes without movement at a flow rate of 50sccm (Standard Cubic Centimeters per Minute) with a power of 100W, and under a pressure of 6.10^{-2} mbar. During the whole process the gas used is Argon (Ar).

Before the actual spraying, a pre-spraying is carried out to remove the oxidized part of the copper in order so that the clean copper can be deposited on the substrate. The power supplied

required for this pre-spraying step is 65W, it is done with argon at a flow rate of 50sccm under a pressure of 5.10-3 mbar. This stage lasts 3 minutes.

The target is copper, with a DC deposit type in our case. The spraying is carried out under the same conditions as the pre-spraying but, unlike the sweeping which is done to make the deposition layer uniform throughout the space of the substrate. This spraying allows to deposit 300nm to 500nm thick layers. Electroplating then increases the copper layer deposited by sputtering only on the parts of the substrate coated with this metal. The thicknesses obtained with this technique range from a few µm to several hundred µm. The deposit speed and the uniformity of the deposits depend on the current density, the composition of the electrolyte, the agitation and recirculation of the electrolyte, the type of polarization (continuous, pulsed), etc.

The part to be covered is then placed in a basin containing a metal salt in solution, i.e. electrolyte based on copper sulfate (CuSO4, 5H2O which dissolves to form a solution of Cu^{2+}-aq + SO_4^{2-}aq) and sulfuric acid H2SO4. In this solution are immersed two electrodes connected to a power source: a pure copper bar connected to the positive pole plays the role of the anode, the sample to be covered connected to the negative pole thus playing the role of the cathode. Fig.2. shows the state of the sample before and after plating.

a) **b)**

Figure 2. Sample a) before electroplating b) after electroplating

B) Realization of antennas

A step of photolithography and one of wet chemical etching are carried out to make the opaque or copper mesh antennas. First, the copper film is coated by centrifugation with a layer of positive photosensitive resin. Then the sample is exposed to ultra violet (UV) light from an insulator through a plastic photomask. After developing the exposed photosensitive resin, the Cu and Ti films are chemically etched. The titanium sublayer is only used here to ensure the strong adhesion of the copper overlayer to the glass substrate. These two processes

make it possible to transfer the antenna geometry to the surface of the synthesized metallic thin layers.

Mesh antennas are characterized by copper lines of width s and pitch p. The mesh, the technology available in our laboratory and the cost of production led us to minimal width grid of around 100µm. The size of the gap between the grids depends on the transparency T and the resistance per square $R_s^{'}$ to obtain. The figure of merit F_0M reflects the performance of the structure, i.e., a good compromise between the resistance per square and the figure of merit has to be found.

- For a square mesh :

$$T(\%) = \left(\frac{p-s}{p}\right)^2 .T_{sub}(\%) \tag{4}$$

$$R_s^{'} = \frac{p}{s}R_s = \frac{p}{s}\frac{1}{e.\sigma} \tag{5}$$

$$F_0M = \frac{Z_0 \times e}{2\rho}\frac{p-s}{p} \tag{6}$$

Where p and s are dimensions defined as in figure 2 and Tsub is the optical transparency of the substrate

- For a rectangular mesh :

$$T(\%) = \left(\frac{p_x-s_x}{p_x}\right) \times \left(\frac{p_y-s_y}{p_y}\right).T_{sub}(\%) \tag{7}$$

$$R_{sx}^{'} = \frac{p_x}{s_y}R_s \; ; \qquad R_{sy}^{'} = \frac{p_y}{s_x}R_s \tag{8}$$

The merit factor according to the two dimensions then becomes:

$$\mathrm{F_0M_x} = \frac{\mathrm{Z_0 \times e}}{2\rho}\frac{\mathrm{p_x - s_x}}{\mathrm{p_x}} \tag{9}$$

$$\mathrm{F_0M_y} = \frac{\mathrm{Z_0 \times e}}{2\rho}\frac{\mathrm{p_y - s_y}}{\mathrm{p_y}} \tag{10}$$

Where p_x, p_y, s_x, s_y are the horizontal and vertical components of p and s.

Table 1. Mesh parameters and related theoretical antenna characteristics.

Theoretical values	Antenna 1	Antenna 2	Antenna 3
	Ground plane (60mm x 72 mm)		
Pitch p_x/p_y (µm)	0	1123/1050	2115/2140

Strip widh s (µm)	0	100	100
Sheet resistance R_{sx}/R_{sy} (Ω/sq)	0.0026	0.029/0.027	0,055/0.0556
Optical transparency T(%)	0	75,82%	83,55%
Feeding line 2.3mm			
Pitch p_x/p_y (µm)	0	1060/1100	1060/1100
Strip widh s (µm)	0	100	100
Sheet resistance R_{sx}/R_{sy} (Ω/sq)	0.0026	0.0275/0.0286	0.0275/0.0286
Optical transparency T(%)	0	75.74%	75.74%
Patch (24mm x 20mm)			
Pitch p_x/p_y (µm)	0	1150/1105	1150/1105
Strip widh s (µm)	0	100	100
Sheet resistance R_{sx}/R_{sy} (Ω/sq)	0,0026	0.03/0.0287	0.03/0.0287
Optical transparency T(%)	0	76.40%	76.40%

To estimate the performance that can be achieved for mesh antennas made with this technology, two mesh antennas (mesh on radiating surface and ground plane), with different mesh sizes on the ground plane, have been designed and compared to an opaque antenna used as a reference (see table 1).

Antennas 2 and 3 have the same feed line and the same radiating element, they differ in the grid pitch of their ground plane. This choice comes from the objective of improving transparency by modifying the mesh of the widest metallization. Due to the mismatch between the dimensions of the antenna and the mesh parameters above, the shape of the mesh is rectangular (see Antennas 2 and 3).

All the circuit values of the equivalent models are listed in Table 2.

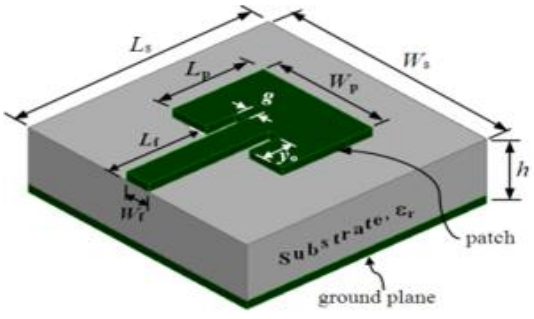

Figure 3. Microstrip patch antenna ***[8]***

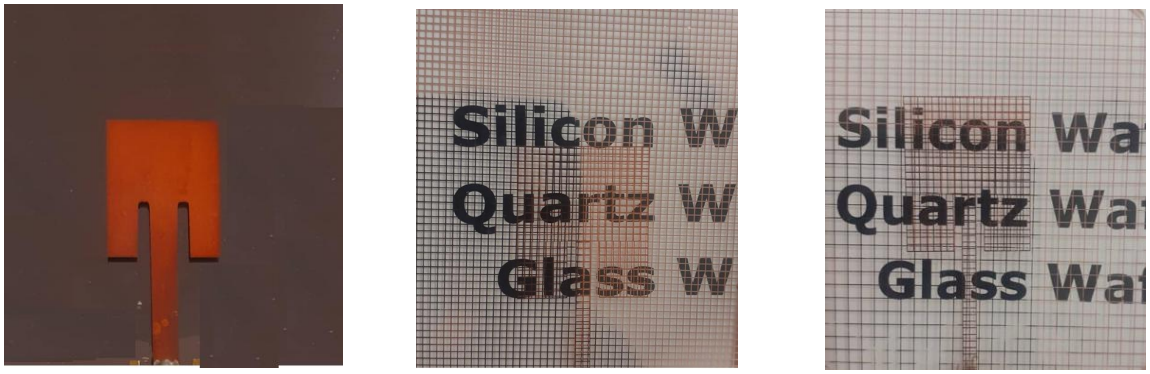

a) **b)** **c)**

Figure 4. Fabricated antennas a) opaque antenna b) transparent antenna 1 c) transparent antenna 2

Table 2. Antennas dimensions

	Antenna	Ground plane	Feed line	Substrate	Recesses
Length (mm)	24 (L_p)	60 (L_s)	24 (L_f)	72 (L_s)	9 (y_0)
Width (mm)	20 (W_p)	60 (W_s)	2.3 (W_s)	60 (W_s)	1.3 (g)
Thickness (mm)	0.0065	0.0065	0.0065	1.1 (h)	0.0065

IV. Simulation and Measurement Results - Discussion

A) Reflection coefficient

Table 3 and Figure 5 compare measured and HFSS-simulated S-parameters of each antenna. S parameters were measured on a vector network analyzer (VNA).

We observe a good agreement between them. A slight shift exists and deformation between them is due to a slight modification of the conductive lines' dimensions of the antennas during wet etching, the roughness of the deposition surface and to measurements uncertainties. Antenna 3, with the most transparent ground plane presents the widest 10dB-bandwidth, around 2.10%, with the lowest matching level (S11 = -12.78dB).

Table 3. Result of simulation and measurement of f_0, S_{11} and Bw of the antennas

	Antenna 1	Antenna 2	Antenna 3
Simulation f_0 (GHz)	2.99	2.84	2.808
Measured f_0 (GHz)	2.98	2.86	2.8
Simulation Bw (%) -10dB	1.37	1.73	2.2
Measured Bw (%) -10dB	1.30	1.60	2.10

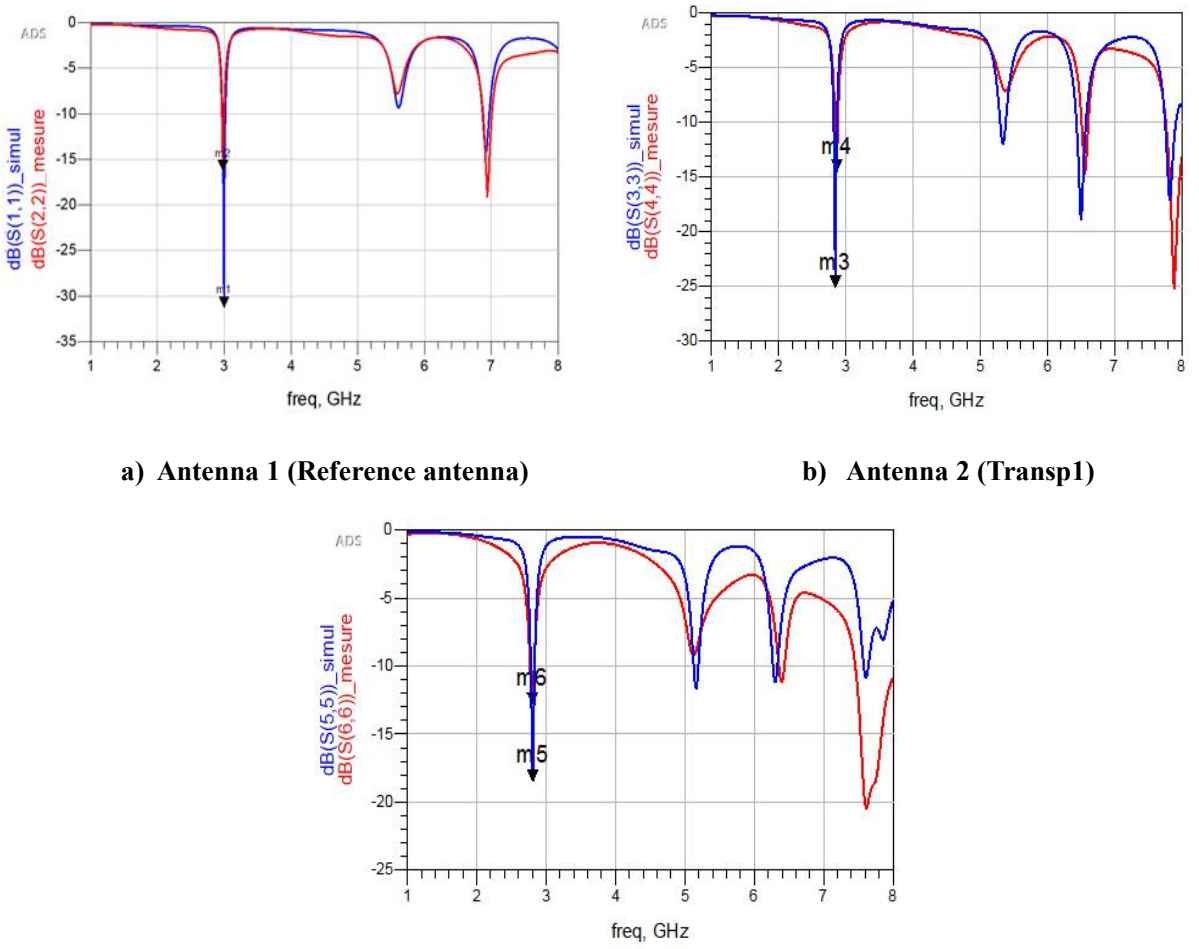

a) Antenna 1 (Reference antenna)

b) Antenna 2 (Transp1)

c) Antenna 3 (Transp2)

Figure 5. Simulated and measured reflection coefficients S_{11}

B) Gains and radiation patterns

The simulation of the gains and the radiation patterns was carried out with the Ansoft HFSS software. Gain and radiation pattern measurements were performed in the far-field anechoic chamber of IETR laboratory in Nantes, France. The measured and simulated radiation patterns of the three antennas at their respective resonant frequencies are compared in on Figure.6 and on Table 4. They show a good agreement on the co-polarization. The main difference between them is on the cross-polarization levels, around 20dBi. This difference may be due to the characteristics of the conductive glue used for the connector.

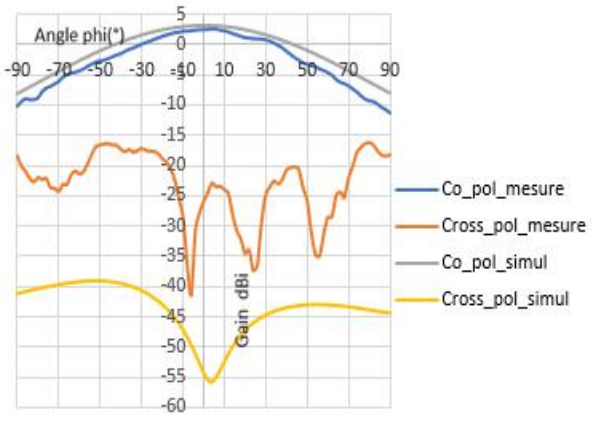

a) Opaque antenna Plan E

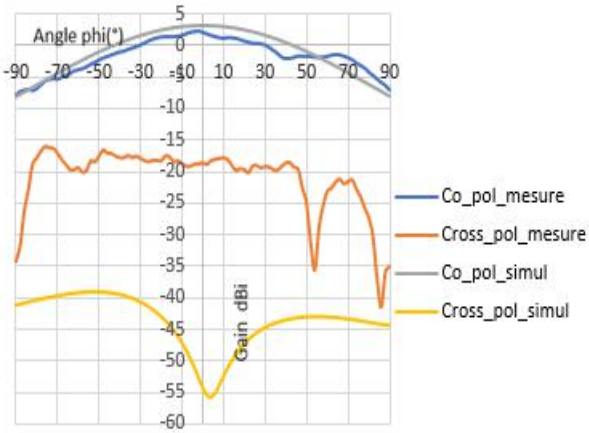

b) Opaque antenna Plan H

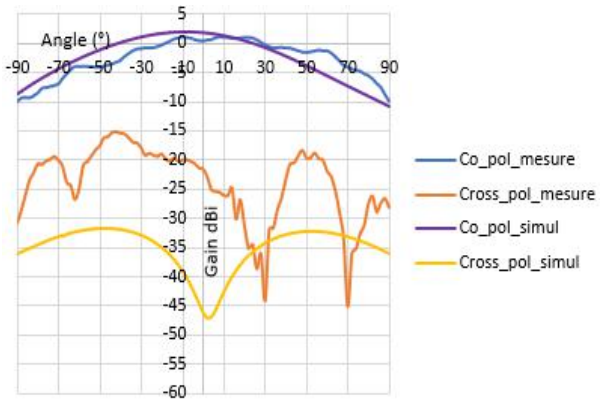

c) Antenna 2 (Transp1) Plan E

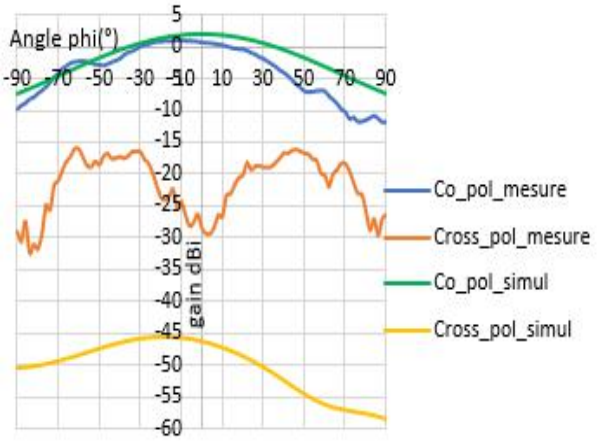

d) Antenna 2 (Transp1) Plan H

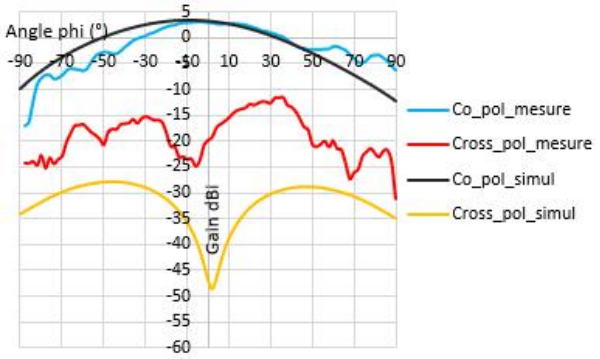

e) Antenna 3 (Transp2) Plan E

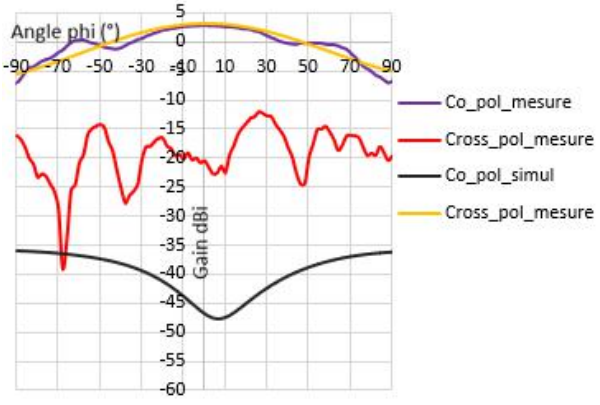

d) Antenna 2 (Transp3) Plan H

Figure 6. Antenna radiation pattern

In addition, measured radiation patterns were affected by various factors: connectors that were cold soldered with conductive glue; the roughness on the surface of the metal deposit; the non-uniformity of the metal thickness.

Table 4. Gain values, simulation and measurement

	Antenna 1	Antenna 2	Antenna 3
Simulation gain (dBi)	3	1.96	3.27
Measured gain (dBi)	2.3	1.8	3.22

The differences between the simulated and measured gains are due to manufacturing and measurement uncertainties.

The maximum measured gain level with antenna 3 is around 3.22dBi at 2.8 GHz while antenna 2 has the lowest gain of around 1.8dBi in Co polarization at 2.86GHz. The difference between the gain in co-polarization and in cross-polarization is greater than 20dBi in measurement than in simulation. Antenna 3 has the best performance in terms of bandwidth, transparency and gain compared to the other two antennas

The optical transparency in the visible of each antenna was measured with using a UV / Visible spectrophotometer, it is between around 60% for antenna 2 and 73% for antenna 3. The difference between theoretical and experimental optical transparency can be due to a defect in alignment, has a direct impact on the optical transparency of the antenna (Figure.7).

With a perfect alignment of the metal bands of the two mesh layers, the optical transparency of the antenna must be optimized as shown in Figure 4c. Usually, two mesh layers cannot be aligned precisely along the entire length of the substrate due to the pitches being slightly different and the mesh not starting at the same location on both sides of the antenna. In cases where higher optical transparencies are required, it is possible to use larger meshes when the thickness of the conductive layer is increased to maintain the same resistance per square [9].

a) **b)** **c)**

Fig. 7. Examples of three different geometric positions of the meshed patterns [10]

a) Rotation of one meshed pattern; b) Translations of one meshed pattern

c) Perfect alignment of the meshed patterns

V. CONCLUSION

The optical, electrical and microwave performance of two see-through antennas using conductive copper films printed on the transparent substrate, borofloat 33 glass, are investigated in this paper. One of them has the same mash size for the radiating element and for the ground plane, but the other has a different ground plane a more transparent. They are compared to an opaque reference antenna.

A simulation technique to size mesh antennas, and simulate them from an opaque one by modifying the metallization thickness and the dielectric permittivity has been presented.

The results show that, with mesh patterns, an antenna with low visual impact has electromagnetic performance similar to that of an opaque antenna, the measured gains and radiation patterns are very close between opaque and mesh antennas. The wire mesh copper antenna with the most transparent ground plane has the best characteristics: a sheet resistance as low as 0.028 Ohms/sq with a gain equal to 3.22dBi, whereas the opaque antenna gain is 2.26dBi at 2.99GHz, while maintaining high optical transparency (73%) in the visible light spectrum. This solution allows us to design and manufacture transparent antennas with microwave performance very close to that of conventional and opaque antennas. However, transparent antennas made with such a material exhibit high microwave performance compared to those produced from metallic, TCO or multilayer ultrafine solutions.

ACKNOWLEDGEMENT

The research is supported by the government of Mali as part of the Training of Trainers Program.

References

[1] Y. Kim, C. Lee, S. Hong, C. W. Jung, et Y. Kim, « Design of transparent multilayer film antenna for wireless communication », *Electronics Letters*, vol. 51, nº 1, p. 12-14, 2015, doi: 10.1049/el.2014.3831.

[2] T. Minami, « New n-Type Transparent Conducting Oxides », *MRS Bulletin*, vol. 25, nº 8, p. 38-44, août 2000, doi: 10.1557/mrs2000.149.

[3] Y. Zhou et R. Azumi, « Carbon nanotube based transparent conductive films: progress, challenges, and perspectives », *Science and Technology of Advanced Materials*, vol. 17, nº 1, p. 493-516, déc. 2016, doi: 10.1080/14686996.2016.1214526.

[4] C. Guillén et J. Herrero, « TCO/metal/TCO structures for energy and flexible electronics », *Thin Solid Films*, vol. 520, nº 1, p. 1-17, oct. 2011, doi: 10.1016/j.tsf.2011.06.091.

[5] S. Hong, Y. Kim, et C. W. Jung, « Transparent UWB Antenna with IZTO/Ag/IZTO Multilayer Electrode Film », *International Journal of Antennas and Propagation*, vol. 2016, p. e6751790, oct. 2016, doi: 10.1155/2016/6751790.

[6] A. Martin, X. Castel, M. Himdi, et O. Lafond, « Mesh parameters influence on transparent and active antennas performance at microwaves », *AIP Advances*, vol. 7, nº 8, p. 085120, août 2017, doi: 10.1063/1.4985746.

[7] « Borosilikatglas BOROFLOAT® - Downloads | SCHOTT AG ». https://www.schott.com/borofloat/english/download/index.html (consulté le 27 mars 2021).

[8] E. Hamad, « Design and Implementation of Dual-Band Microstrip Antennas for RFID Reader Application », *Ciência e Técnica Vitivinícola*, vol. 29, p. 2-10, sept. 2014.

[9] J. Hautcoeur *et al.*, « Transparency and electrical properties of meshed metal films », *Thin Solid Films*, vol. 519, nº 11, p. 3851-3858, mars 2011, doi: 10.1016/j.tsf.2011.01.262.

[10] J. Hautcoeur, L. Talbi, K. Hettak, et M. Nedil, « 60 GHz optically transparent microstrip antenna made of meshed AuGL material », *Microwaves, Antennas & Propagation, IET*, vol. 8, p. 1091-1096, oct. 2014, doi: 10.1049/iet-map.2013.0564.